Simulation of acoustic lens influence on wavefront shaping

Tomasz NOWAK, Andrzej DOBRUCKI [ID]

Department of Acoustics, Multimedia and Signal Processing, Wrocław University of Science and Technology, Wybrzeże Wyspiańskiego 27, 50-370 Wrocław , Poland

Corresponding author: Tomasz NOWAK, email: t.nowak@pwr.edu.pl

Abstract The main objective of presented study is to examine the influence of an acoustic lens on shape of the wavefront. To conveniently illustrate the difference between acoustic pressure wave propagation with and without the lens, an isodynamic transducer was chosen as a source. This kind of loudspeaker generates flat wavefront as a result of approximately uniform distribution of speed and phase on the entire diaphragm. The designed lens consisted of a matrix of individual waveguides. Manipulation of size and position of output matrix in relation to input matrix allowed for achieving the desired waveguide length distribution. Differences in lengths of lens's channels resulted in wavefront delay distribution at the output matrix. A numerical model of transducer and waveguide matrix was created to evaluate the behaviour of acoustic pressure wave propagation trough the designed lens. With stationary study, a spatial pressure distribution was calculated, in the near field and far field, in hemisphere in front of the lens as well as in hemisphere in front of just the transducer. The differences in wavefront shapes between the two cases were clearly visible in comparisons, confirming the expected pressure wave delay distribution of the lens. The resulting wavefront curvature was compared to the assumed one in theoretical design. Results of those comparisons proved the possibility of influencing the wavefront shape, by manipulating the output matrix with some caveats discussed in the paper. The data from numerical calculation of pressure propagation allowed for visualizing calculated sound pressure level distribution, adding the directivity evaluation to the comparisons.

Keywords: transducers, waveguides, pressure acoustics, numeric methods, simulation.

1. Introduction

The science and engineering behind the design of electroacoustic transducers and loudspeaker devices faces complicated limitations resulting from the mismatch of radiation angles of sources and the shapes of their wave fronts. The physical dimensions and placement of speakers, including loudspeaker devices, in relation to the generated wavelengths are related to the occurrence of interference on the surface of the wave front. As a result of phase and amplitude mismatch, a sound source is created that distorts the acoustic signal as a function of frequency. The solution to the above-mentioned problems would be the possibility of freely shaping the wave fronts, creating a coherent source with given parameters of radiation angles and amplitude response in space. For this purpose, acoustic lenses that discretize the wave front can be used.

Any section of the surface in the acoustic field can be divided into unit fragments, forming a matrix located at the input of the lens. The output of the lens is a matrix with the same number of cells but with a different spatial orientation [1, 2]. The cells of the input and output matrix are connected by channels. The difference in the arrangement of cells between two matrices introduces a difference in the length of the channels connecting them, as a result of which the phase delay in each of the output cells can be adjusted.

A proposal for a discretizing structure that allows to regulate the curvature of the generated wave in two planes is shown in Fig. 1, where the output matrix is larger than the input one. Scaling the size and output position of the matrix in both directions allows the wave front to be shaped as flat, cylindrical, ellipsoidal, and other spatial curvatures [3].
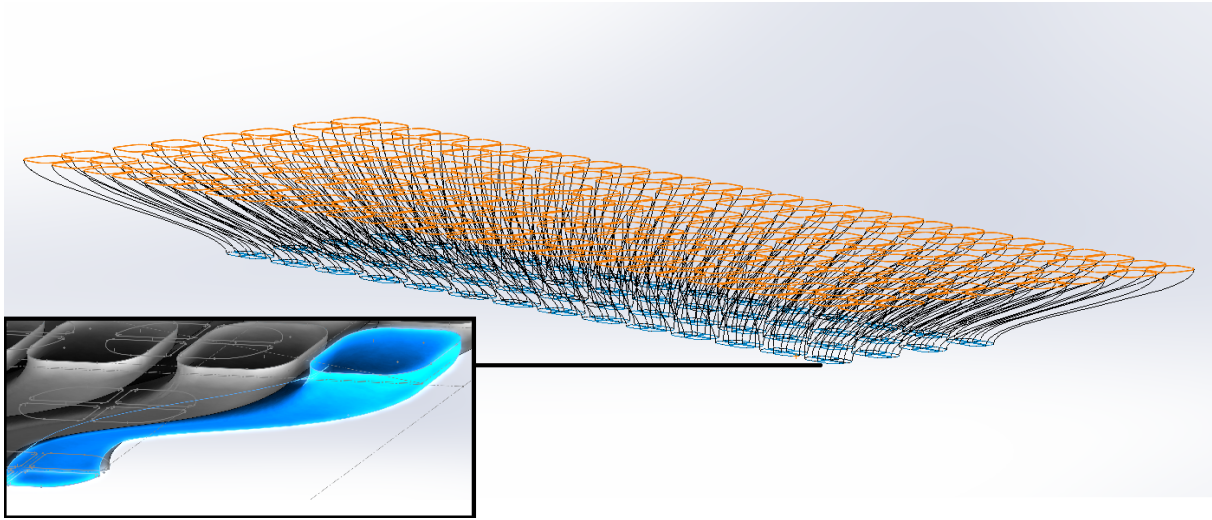
Figure 1. Input (blue) and output (orange) matrixes of the proposed lens,
with visualization of a single channel.

2. Transducer under consideration

Every loudspeaker has its specific radiation pattern, the directivity increases with diaphragm size and frequency, resulting in higher *kl* values (1). The shape of diaphragm, its material properties and location of excitation source, all determine the non-linear behaviour at higher frequencies, where movement of the surface is non-uniform, further complicating the radiation pattern with increasing frequency. For a rectangular piston with uniform velocity distribution (characterized by the value *Q* and efficiency of a single point source), the sound pressure is given by:

$$p(r, \theta_1, \theta_2) = \frac{\rho_0 c |Q| k}{2\pi r} \frac{\sin \frac{kl_1 \sin \theta_1}{2}}{\frac{kl_1 \sin \theta_1}{2}} \cdot \frac{\sin \frac{kl_2 \sin \theta_2}{2}}{\frac{kl_2 \sin \theta_2}{2}}, \tag{1}$$

where *p* is the far-field pressure radiated by a baffled rectangular piston depends on the dimensions of the piston, the frequency (through the wavenumber *k* and the directions *θ₁* and *θ₂*).Directivity is the product of the directivity of continuous linear sources of length *l₁* and *l₂* (in this case these are the lengths of the sides of the rectangle), and angles *θ₁* and *θ₂* are the angles between normal to the piston surface and the projections connecting the center of the piston to the observation point in the far field, on planes perpendicular to the piston surface and parallel to *l₁* and *l₂* respectively [4].

An example of transducer, which is characterized by uniform distribution of velocity on the entire diaphragm, is an isodynamic loudspeaker. It is the simplest to simulate and generates a flat wavefront by its principle of operation. This type of transducer can be used in wide range of frequencies, if the diaphragm size is substantial. The drawback of using large radiating area to create acoustical pressure at wavelengths the fraction of its size is high directivity, increasing with frequency. Solution to this problem comes in form of a lens that is able to transform the flat acoustic wavefront into a curved one. This will result in lowering directivity for high frequencies, because the curved wavefront will behave similarly to the one radiated from a fraction of pulsating sphere, rather than an oscillating flat surface [5]. The pulsating sphere is omnidirectional, the far-field pressure is not related to the direction *θ*:

$$\mathbf{p}_{ext}(r) = \frac{a}{r} v_r \rho_0 c \frac{-ika}{1-ika} \exp(ik(r-a)), \tag{2}$$

where $\mathbf{p}_{ext}$ is the far-field pressure radiated at a distance *r* from the center of the pulsating sphere of radius *a.*

3. Geometry guidelines

In preparation for simulation, a model of lens has to be designed. The input matrix derived from technical drawings of selected isodynamic transducer. The output matrix was scaled up by a factor of 1.372 in vertical direction (longer dimension of the transducer) and by a factor of 2.057 in horizontal direction (shorter dimension of the transducer). With lens thickness of 15 mm, those factors were calculated to achieve input-output cell distance distribution approximating wavefront with curvature radius of X=260 mm in horizontal direction and Y=580 mm in vertical direction. The actual delay distribution along the axis of symmetry is parabolic, as a result of linear output matrix scaling. The resulting wavefront of this lens should be a fraction of an ellipsoid [3].

3.1. 3D model

To create the lens geometry, a parametric model of the structure was developed in CAD software. The variables of this model consisted of: output matrix scaling factors, lens thickness, wall thickness between the channels, channel shape and tangency, etc. The channels connecting input with output cells were modelled with splines as guidelines, with ends perpendicular to the surface of those cells. Prepared geometry was exported to the simulation software.

4. Simulation model

The model was prepared for finite element method (FEM) study. Because of limited computing resources, the geometry was encapsulated in a sphere, 500 mm in diameter. Larger distances as well as possibility of switching to BEM study required substantially more than a terabyte of system memory, which was out of reach for this research. Volume of this encapsulation was divided into tetrahedral elements, with maximum distance between the nodes defined as 1/5 of studied wavelength, what is a prerequisite for performing calculations. It was a largest distance necessary to achieve convergence. Top half of the studied sphere consisted of the lens in baffle, bottom half encapsulated just the diaphragm (input matrix) in baffle. The baffles reached the encapsulating sphere, creating independent simulations of lensed and lensless loudspeaker. The described configuration is shown in Fig. 2.
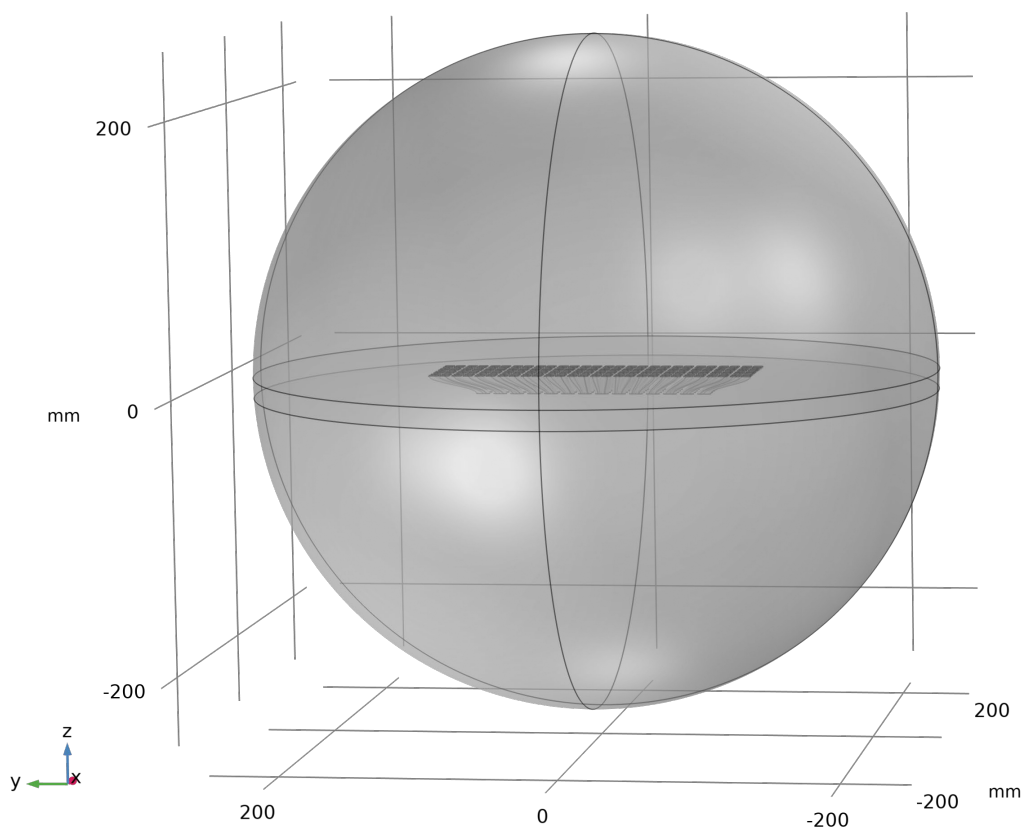

Figure 2. Simulation geometry configuration, transparent for sphere interior visualization.

4.1. Physics interface

The physics interface solves the Helmholtz equation in the frequency domain for given frequencies. An acoustics model can be part of a larger multiphysics model that describes, for example, the interactions between structures and acoustic waves. This physics interface is suitable for modeling acoustics phenomena that do not involve fluid flow (convective effects). The sound pressure p, which is solved for in pressure acoustics, represents the acoustic variations (or acoustic perturbations) to the ambient pressure. In the absence of flow, the ambient pressure p_A is simply the static absolute pressure. The governing equations and boundary conditions are formulated using the total pressure p_t with a so-called scattered field formulation. In the presence of a background pressure field defining a background pressure wave p_b (this could, for example, be a plane wave), the total acoustic pressure p_t is the sum of the pressure solved for p (which is then equal to the scattered pressure p_s) and the background pressure wave: $p_t = p+p_b$. The equations then contain the information about both the scattered field and the background pressure field [6]. For further simulation description, the following table lists the names and SI units for the most important physical quantities in the pressure acoustics, frequency domain interface (Table 1).

Table 1. Pressure acoustics, frequency domain interface physical quantities.

Quantity	Symbol	SI Unit
Pressure	p	Pascal
Total pressure	p_t	Pascal
Background pressure	p_b	Pascal
Scattered pressure	p_s	Pascal
Density (quiescent)	ρ or ρ_c	kilogram/meter³
Frequency	f	Hertz
Wave number	k	1/meter
Dipole domain source	q_d	newton/meter³
Monopole domain source	Q_m	1/second²
Speed of sound	c or c_0	meter/second
Specific acoustic impedance	Z or Z_{sp}	pascal-second/meter
Acoustic impedance	Z_{ac}	pascal-second/meter³
Normal acceleration	a_n	meter/second²
Normal velocity	v_n	meter/second
Source location	x_0	meter
Unit vector, normal to wave direction	n	(dimensionless)

4.2. Geometry definitions

To simulate the acoustic pressure propagation with finite element method, the previously mentioned interface was selected for all of the domains in the model, with assigned temperature T = 293.15 K and absolute pressure of p_A = 0.1 MPa. It is defined with following wave equation (3):

$$\nabla \cdot \left(-\frac{1}{\rho}(\nabla p_t - q_d) \right) - \frac{k_{eq}^2 p_t}{\rho} = Q_m, \tag{3}$$

where $k_{eq}^2 = \left(\frac{\omega}{c}\right)^2$.

All of the surfaces in the imported model were grouped into active radiating area domain and acoustic wave boundary domain, both were assigned with initial value of pressure as p = 0 Pa. The former consisted of surfaces corresponding to active radiating area of input matrix, with defined uniform normal velocity definition, described with wave equation

$$-n \cdot \left(-\frac{1}{\rho}(\nabla p_t - q_d)\right) = i\omega n \cdot v_0, \tag{4}$$

where v_0 was assigned initial values of 0 in x and y directions and value of 0.1 m/s in z direction.

The latter consisted of all of the remaining surfaces (channel walls, front baffle and rear baffle), which were defined as hard acoustic boundary

$$-n \cdot \left(-\frac{1}{\rho}(\nabla p_t - q_d)\right) = 0. \tag{5}$$

The surface of sphere which encapsulates study volume was defined as "spherical wave radiation" instead of an acoustic boundary, to simulate radiation of the pressure to the outside 'void':

$$-n \cdot \left(-\frac{1}{\rho}(\nabla p_t - q_d)\right) + \left(ik_{eq} + \frac{1}{r_{rf}}\right)\frac{p}{\rho} - \frac{r_{rf}\Delta_{\parallel}p}{2\rho(1 + ik_{eq}r_{rf})} = Q_i, \tag{6}$$

where $r_{rf} = |(x - r_0)|$, r_0 is a radiating source field location.

4.3. Calculation method

When choosing the calculation method, the hardware limitations were taken into account. The direct solver requires substantial amount of operation memory, more than was available for this paper. To limit RAM dependency, an iterative, stationary solver was chosen. To achieve accurate results, the relative tolerance was set to 0.001. The solver was "fully coupled", which means solving for all of the variables at the same time until achieving convergence. The solver of choice was "GMRES with GMG", which uses the generalized minimum residual iterative solver with a geometric multigrid preconditioner. This method is typically faster than the direct solver and uses less memory for large 3D models.

5. Results

The calculations were made in frequency domain, for frequencies: 1; 2; 4; 8; 16 [kHz], resulting in spatial acoustic pressure distribution within the specified sphere (Fig. 3). Results were plotted in zx plane ('horizontal' radiation of shorter side of the lens) and in zy plane ('vertical' radiation of longer side of the lens). On every plot, the upper semicircle ($z > 0$ mm) contains pressure distribution of the loudspeaker with lens, the lower semicircle ($z < -15$ mm) contains pressure distribution of the loudspeaker without the lens. For practical reasons, this paper will focus on high frequencies, which clearly illustrate the influence of the studied lens.
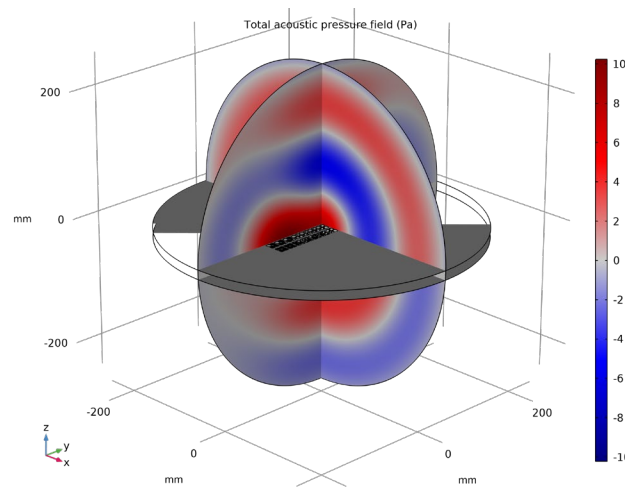

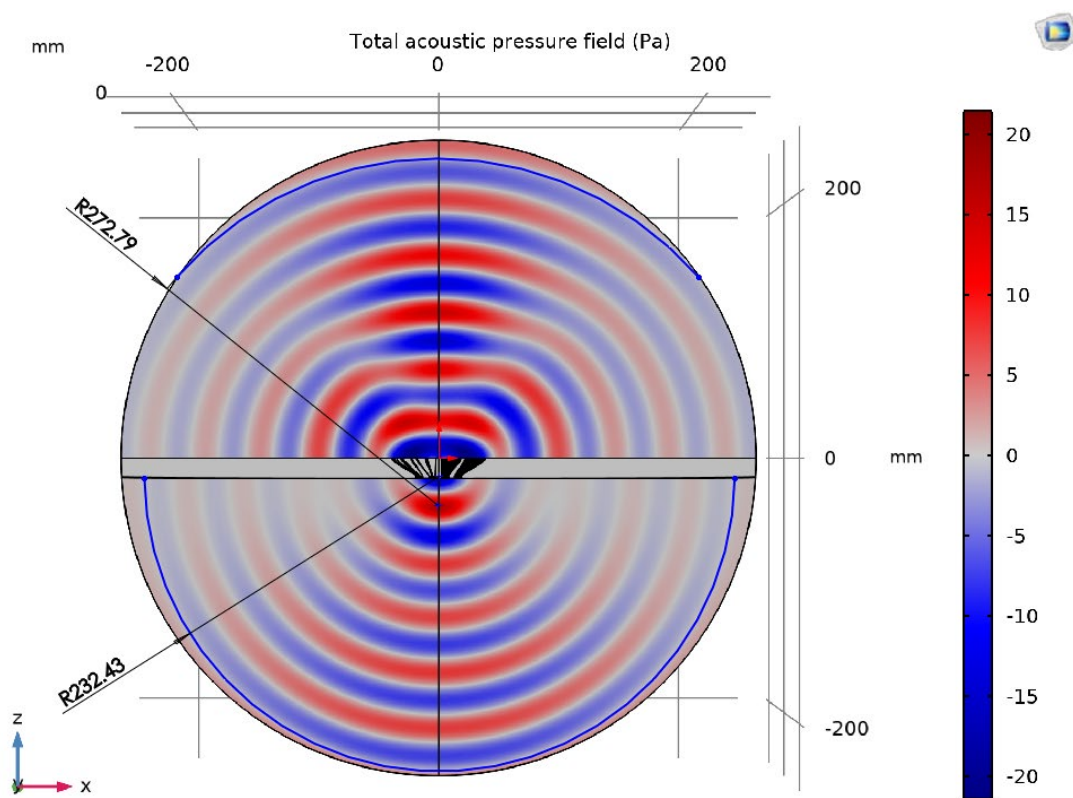**Figure 3.** Total acoustic pressure field, spatial arrangement of the results.

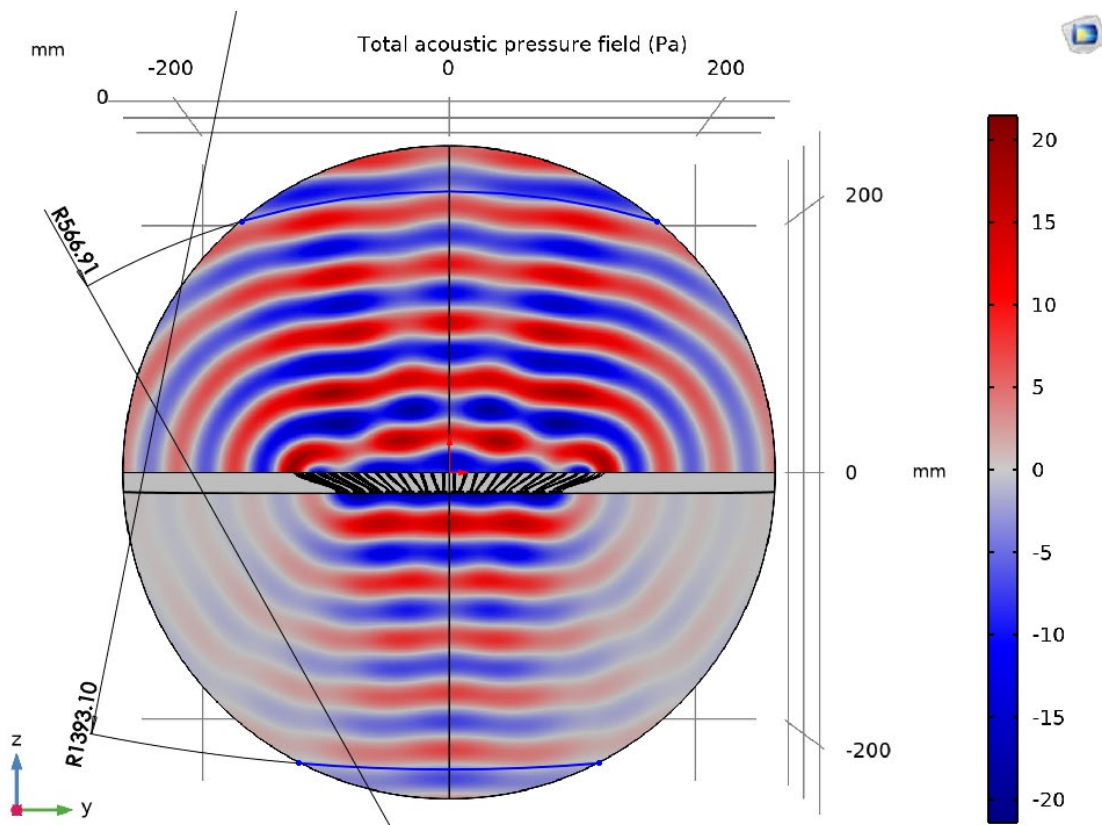**Figure 4.** Simulation result, f = 8 kHz, 'horizontal' radiation.

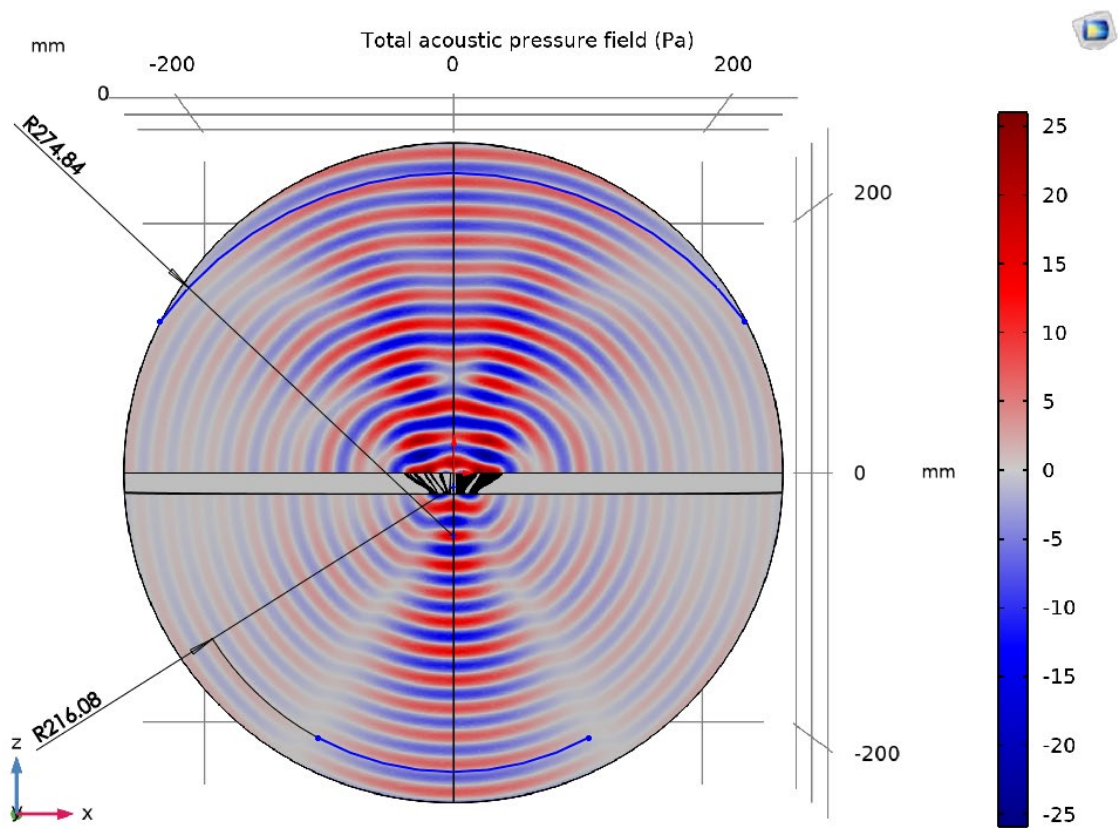**Figure 5.** Simulation result, f = 8 kHz, 'vertical' radiation.

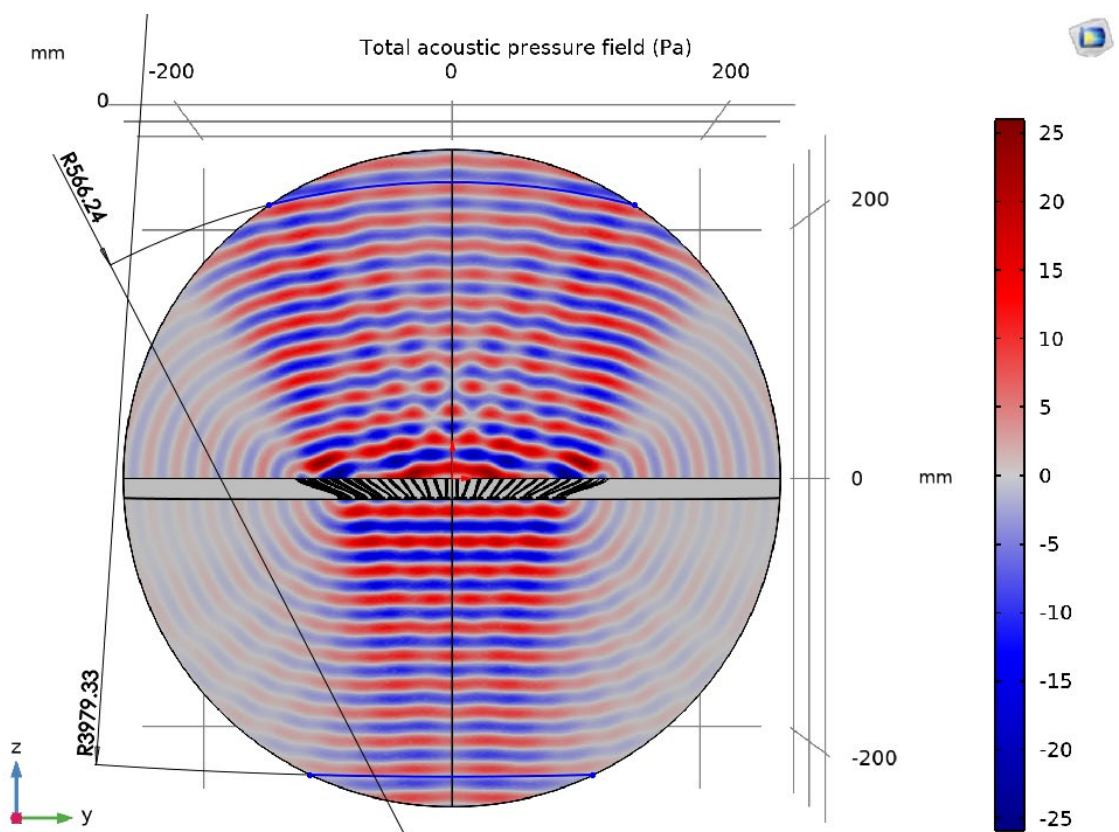**Figure 6.** Simulation result, f = 16 kHz, 'horizontal' radiation.

Figure 7. Simulation result, f = 16 kHz, 'vertical' radiation.

The acoustic wavefront curvature was approximated by fitting the closest matching arc to the pressure distribution shape near the calculation sphere (to minimize nearfield phenomena). The radii of those arcs were determined for each case and grouped in Tab. 2, 3.

Table 2. Approximated radii of simulated acoustic wavefronts, 'horizontal' radiation.

Frequency [kHz]	Radius without lens [mm]	Radius with lens [mm]	Designed radius [mm]
1	250	250	260
2	243	243	260
4	210	246	260
8	232	273	260
16	216	275	260

Table 3. Approximated radii of simulated acoustic wavefronts, 'vertical' radiation.

Frequency [kHz]	Radius without lens [mm]	Radius with lens [mm]	Designed radius [mm]
1	232	256	580
2	259	413	580
4	391	529	580
8	1393	567	580
16	3979	566	580

6. Conclusions

The simulation results (Fig. 5 and 7) show significant influence on the acoustic wavefront shape, radiated by an isodynamic transducer, which was the goal of this research. The lens effectiveness is related to it's size, minimal influence on wavefront shape can be observed in 'horizontal', shorter dimension (Fig. 4 and 6). Pressure wave propagation is split and delayed through the lens channels of distributed length, resulting in curved wavefront at the output matrix. The radius of this curvature can be controlled in the geometric design stage, the differences between curvature radius in design assumptions and simulated one allows for relative accuracy of over 90%. The influence of lens is related to the output matrix size in relation to wavelength, like every other type of source. For wavelengths smaller than lens dimensions, the radiated wavefront curvature radius is consistently close to the assumed one in function of frequency (Tab. 2, 3).

This behaviour has potential to result in constant directivity loudspeaker device, rivalling substantially larger horn-loaded solutions. Presented solution minimizes the distance between loudspeaker and output, reducing the size of loudspeaker device, as well as introduced acoustic delay in comparison to conventional waveguides. Predictable wavefront curvature achieved by discussed type of lens could also be used in larger arrays of lenses, providing summation of sources with little to none destructive interference between them. This feature could allow for designing a specific curvature and size of the source, with multiple loudspeakers behaving as a single transducer.

As mentioned before, the lens model was designed around an actual loudspeaker, which opens possibility of manufacturing a prototype for future measurements. Collected data will be compared to presented simulations, evaluating their correctness.

Additional information

References

1. T. Dahl, J. L. Ealo, K. Papakonstantinou, J. F. Pazos; Design of Acoustic Lenses for Ultrasonic Human-Computer Interaction; IEEE International Ultrasonics Symposium, 1 October 2011; DOI:10.1109/ULTSYM.2011.0017
2. V. Berstis; 3D printed acoustic lens for dispersing sound; J. Audio Eng. Soc., 2018, 66 (12), 1082–1093
3. T. Nowak, A. Dobrucki; Koncepcja matrycy falowodowej do kształtowania frontu fali akustycznej (in Polish:); XIX Międzynarodowe Sympozjum Nowości w Technice Audio i Wideo NTAV2022, Wrocław, Poland, 13-15.10.2022; InfoArt, 2022, 18-19
4. Z. Żyszkowski; Podstawy elektroakustyki (in Polish); WNT, 1984
5. A. Dobrucki; Przetworniki elektroakustyczne (in Polish); WNT; 2007
6. COMSOL documentation website; URL: https://doc.comsol.com/5.5/doc/com.comsol.help.aco/aco_ug_pressure.05.002.html (accessed on 2023.07.10)